



**HAL**  
open science

## Open access segmentations of intraoperative brain tumor ultrasound images

Bahareh Behboodi, Francois-xavier Carton, Matthieu Chabanas, Sandrine de Ribaupierre, Ole Solheim, Bodil Munkvold, Hassan Rivaz, Yiming Xiao, Ingerid Reinertsen

### ► To cite this version:

Bahareh Behboodi, Francois-xavier Carton, Matthieu Chabanas, Sandrine de Ribaupierre, Ole Solheim, et al.. Open access segmentations of intraoperative brain tumor ultrasound images. Medical Physics, 2024, 10.1002/mp.17317 . hal-04661871

**HAL Id: hal-04661871**

**<https://hal.science/hal-04661871v1>**

Submitted on 25 Jul 2024

**HAL** is a multi-disciplinary open access archive for the deposit and dissemination of scientific research documents, whether they are published or not. The documents may come from teaching and research institutions in France or abroad, or from public or private research centers.

L'archive ouverte pluridisciplinaire **HAL**, est destinée au dépôt et à la diffusion de documents scientifiques de niveau recherche, publiés ou non, émanant des établissements d'enseignement et de recherche français ou étrangers, des laboratoires publics ou privés.

# Open access segmentations of intra-operative brain tumor ultrasound images

Bahareh Behboodi<sup>1,2,\*</sup>, Francois-Xavier Carton<sup>3,\*</sup>, Matthieu Chabanas<sup>3</sup>, Sandrine de Ribaupierre<sup>4</sup>, Ole Solheim<sup>5,6</sup>, Bodil K. R. Munkvold<sup>5,6</sup>, Hassan Rivaz<sup>1,2</sup>, Yiming Xiao<sup>2,9</sup>, Ingerid Reinertsen<sup>7,8</sup>

<sup>1</sup>Department of Electrical and Computer Engineering, Concordia University, Montreal, Canada

<sup>2</sup>School of Health, Concordia University, Montreal, Canada

<sup>3</sup>Université Grenoble Alpes, CNRS, Grenoble INP, TIMC, F-38000 Grenoble, France

<sup>4</sup>Department of Clinical Neurological Sciences, Schulich School of Medicine and Dentistry, Western University, London, Ontario, Canada

<sup>5</sup>Department of Neurosurgery, St. Olavs Hospital, Trondheim University Hospital, Norway

<sup>6</sup>Department of Neuromedicine and Movement Science, Norwegian University of Science and Technology (NTNU), Trondheim, Norway

<sup>7</sup>Department of Health Research, SINTEF Digital, Trondheim, Norway

<sup>8</sup>Department of Circulation and Medical Imaging, Norwegian University of Science and Technology (NTNU), Trondheim, Norway

<sup>9</sup>Department of Computer Science and Software Engineering, Concordia University, Montreal, Canada

\* These authors share first authorship.

† Corresponding author:

b\_behboo@encs.concordia.ca

(or behboodibahareh@gmail.com)

## Abstract

**Purpose:** Registration and segmentation of magnetic resonance (MR) and ultrasound (US) images could play an essential role in surgical planning and resectioning brain tumors. However, validating these techniques is challenging due to the scarcity of publicly accessible sources with high-quality ground truth information. To this end, we propose a unique set of segmentations (RESECT-SEG) of cerebral structures from the previously published RESECT dataset to encourage a more rigorous development and assessment of image processing techniques for neurosurgery.

**Acquisition and Validation Methods:** The RESECT database consists of MR and intra-operative US (iUS) images of 23 patients who underwent brain tumor resection surgeries. The proposed RESECT-SEG dataset contains segmentations of tumor tissues, *sulci*, *falk cerebri*, and resection cavity of the RESECT iUS images. Two highly experienced neurosurgeons validated the quality of the segmentations.

**Data Format and Usage Notes:** Segmentations are provided in 3D NIFTI format in the OSF open-science platform: <https://osf.io/jv8bk>.

**Potential Applications:** The proposed RESECT-SEG dataset includes segmentations of real-world clinical US brain images that could be used to develop and evaluate segmentation and registration methods. Eventually, this dataset could further improve the quality of image guidance in neurosurgery.

## 42 I. Introduction

43 Gliomas are the most common malignant primary brain tumors originating from glial cells  
44 and are classified into grades 1-4 by the World Health Organization (WHO)<sup>1,2</sup>. Grades 1-  
45 2 are low-grade, while grades 3-4 are high-grade tumors<sup>3</sup>. Surgical resection is a standard  
46 treatment for gliomas, and pre-operative magnetic resonance (MR) imaging is used for tumor  
47 characterization. However, brain tissue deforms during surgery due to factors like edema and  
48 gravity (i.e. brain shift)<sup>4</sup>, rendering pre-operative MR images inaccurate. Acquiring data at  
49 different stages during surgery helps the surgeon better monitor the progress of the tumor  
50 resection and, consequently, operate more precisely. Intra-operative imaging, particularly  
51 intra-operative MR (iMR) and intra-operative ultrasound (iUS) aids surgeons by providing  
52 updated guidance<sup>5,6,7</sup>. While iMR offers superior image quality, it is costly, adds a long  
53 time to the operation, and requires dedicated operating rooms<sup>8,9</sup>. In contrast, iUS is a cost-  
54 effective, flexible, and versatile modality that presents real-time scanning without altering  
55 the surgical workflow<sup>10,11,12</sup>. Due to the easy procedure of acquiring iUS rather than iMR,  
56 several recent studies have demonstrated the use and interest in iUS in neurosurgery<sup>8,11,12,13</sup>.

57 While iUS presents several advantages in the context of brain tumor resection, ultra-  
58 sound (US) images can be difficult to interpret. Non-standard imaging planes and unfamiliar  
59 contrast are major factors limiting the efficient and widespread use of US in neurosurgery.  
60 To mitigate such limitations and fully leverage the advantages of iUS, automated image seg-  
61 mentation of structures such as tumors within iUS images can provide valuable assistance to  
62 neurosurgeons during procedures. Recent automated image segmentation algorithms, such  
63 as deep learning (DL) algorithms have made advancements in brain tumor segmentation  
64 from both US<sup>14,15,16,17</sup> and MR<sup>18,19,20,21</sup> images. However, access to high-quality datasets ex-  
65 pertly annotated is essential for the development and validation of DL algorithms<sup>22</sup>. In the  
66 context of medical imaging, MR images have seen more readily available datasets compared  
67 to other modalities, making them the primary focus for DL algorithm development. The  
68 BRATS challenge, among others, stands out as a prominent dataset with valuable annota-  
69 tions that have significantly contributed to the evolution and refinement of DL algorithms<sup>23</sup>.  
70 Acquiring such data, especially for iUS images, is expensive and rare.

71 Currently, there are only three publicly available datasets that provide iUS brain im-  
72 ages, the BITE dataset<sup>24</sup>, the RESECT database<sup>25</sup>, and ReMIND<sup>26</sup>. The BITE dataset  
73 contains pre- and post-operative MR scans as well as multiple iUS images of 14 patients.  
74 The RESECT database contains pre-operative MR scans and iUS images from 23 patients  
75 with low-grade gliomas. The ReMIND dataset contains 369 pre-operative MR scans, 320 3D  
76 iUS scans, 301 iMR scans, and 356 pre-operative MR segmentations of 114 patients. None of  
77 the abovementioned datasets contain segmentation of anatomical structures in the iUS im-  
78 ages, thereby hindering the development and validation of iUS processing methods. For the  
79 RESECT database, a few research groups have previously conducted segmentations of iUS  
80 images<sup>14,18,27</sup>. However, a portion of these annotations remained inaccessible to the public,  
81 and in some instances, only a small subset of cases was segmented, with limited validation  
82 procedures in place.

83 In this work, we present the most comprehensive and validated expert segmentations of  
84 cerebral structures in iUS images from the RESECT database. The focus of the RESECT-  
85 SEG dataset is on delineating the tumor in pre-resection iUS 3D volumes and identifying the  
86 resection cavity during and after the surgery. To enhance the surgeon’s ability to achieve  
87 more precise tumor resection, *sulci* and the *falx cerebri*, whenever they were within the  
88 field of view, were also delineated. These structures commonly serve as crucial anatomical  
89 references for surgeons, given their clear visibility in iUS images. The following sections  
90 detail the segmentation and validation protocols for all the mentioned structures in the iUS  
91 images and brain tumor segmentation in pre-operative MR images.

## 92 II. Acquisition and Validation Methods

93 In this section, a comprehensive overview of the dataset is presented, along with detailed an-  
94 notations for various anatomical structures, including tumors, resection cavities, *falx cerebri*,  
95 and *sulci*. The annotation process involved the utilization of two primary tools: ITK-SNAP<sup>28</sup>  
96 and 3D Slicer<sup>29</sup>, chosen based on individual preference and familiarity. Furthermore, specific  
97 built-in features of these software platforms were leveraged as necessary, such as smoothing  
98 and interpolation functionalities, to enhance the accuracy and completeness of the annota-  
99 tions. Further elaboration on these tools and their respective functionalities is provided in  
100 the subsequent paragraphs. Given that both ITK-SNAP and 3D Slicer are widely used tools  
101 in the field, the decision to select one over the other was solely based on our inter-group  
102 preferences. It is important to highlight that manual segmentation entails human judgment  
103 and expertise, enabling nuanced interpretation and adjustments tailored to the anatomical  
104 complexities of each case. Consequently, the choice of segmentation software or algorithm  
105 does not introduce bias, as it depends on the proficiency and diligence of the annotators.

### 106 II.A. RESECT Database

107 The RESECT database<sup>25</sup> comprises pre-operative contrast-enhanced T1-weighted and T2  
108 FLAIR MR scans alongside three 3D volumes of iUS scans from 23 patients with low-grade  
109 gliomas (grade 2) who underwent surgeries between 2011 and 2016 at St. Olavs University  
110 Hospital, Trondheim, Norway. The iUS scans were acquired at three different stages of  
111 the procedure: before resection, during resection, and after resection for control. These US  
112 images were captured by an expert surgeon, and the database includes manual neuroanatomy  
113 landmarks, facilitating MR-to-US volume registration and inter-US volume alignment. The  
114 details of the image acquisition procedure can be summarized as follows:

- 115 • Pre-operative MR scans: T1-weighted and T2 FLAIR sequences were acquired on 3T  
116 Magnetom Skyra MR scanners, both with 1 mm isotropic voxel size, except three  
117 patients who underwent the MR imaging on a 1.5T Magnetom Avanto MR scanner  
118 with 1 mm slice thickness.

- Intra-operative US scans: 3D US images collected using a 12FLA-L linear probe of Sonowand Invite neuronavigation system with a frequency range of 6-12 MHz integrated with the NDI Polaris optical tracking system.

## 122 II.B. iUS Tumor Segmentation Protocol

123 Tumoral tissue in US images is typically identified through abnormal echogenicity or texture variations compared to healthy tissue. Echogenicity refers to the level of reflectivity or brightness of tissue on a US image. In this context, variations in echogenicity indicate potential areas of malignancy, allowing medical professionals to identify and examine potential cancerous lesions. In the study, 19 out of 23 cases' iUS images (cases 1 to 23) were segmented, initially following Munkvold et al.'s method<sup>27</sup>. In these cases, initial US volume segmentations were already available. Four cases (cases 24 to 27) without prior iUS segmentations relied on MR segmentations to define the tumor region of interest in iUS images. To be more specific, for these four cases, the MR segmentation served as a starting point to define the region of interest (ROI) for the tumor in the iUS images. Further details of the MR segmentation protocol can be found in the work of Munkvold et al.<sup>27</sup>.

134 In the iUS segmentation protocol, 3D Slicer<sup>29</sup>, a free and open-source medical image analysis software, was employed to perform ground truth segmentations on the acquired iUS images. For cases 24 to 27 that were initiated with MR segmentations due to brain shift during resection surgery, the boundaries of the tumor in the US images and MR tumor segmentations did not align<sup>25</sup>. This discrepancy necessitated the registration of MR tumor segmentations to iUS images using available landmarks from the RESECT database. This registration process effectively mitigated the misalignment of tumor borders between the iUS images and their corresponding MR tumor segmentations. Therefore, for cases 24 to 27, the MR segmentations were imported into the 3D Slicer scene and after the registration step, they were utilized as the initial delineation for iUS.

144 In all cases, to refine the initial 3D US tumor segmentations, the Label Map Smoothing module, an existing feature in 3D Slicer, was employed. Subsequently, the smoothed tumor segmentations were manually fine-tuned to ensure accurate coverage of the tumor region in the iUS image. To facilitate further correction, FLAIR MR images were registered to iUS images since MR images were unaffected by brain-shift effects. These complementary overlays served as guidance for generating more precise iUS tumor segmentations. An illustrative example of tumor segmentation is provided in Fig. 3 (a)-(d).

## 151 II.C. iUS Resection Cavity Segmentation Protocol

152 Resection cavity segmentation in iUS images encompasses the volume where tissue has been resected or retracted during image acquisition. Resection, a surgical procedure characterized by the complete removal of tissue or tumors, contributes to the formation of a distinct three-dimensional space within the brain known as the resection cavity. On the other hand, retraction, another surgical maneuver, entails cutting tissue and displacing it to the side

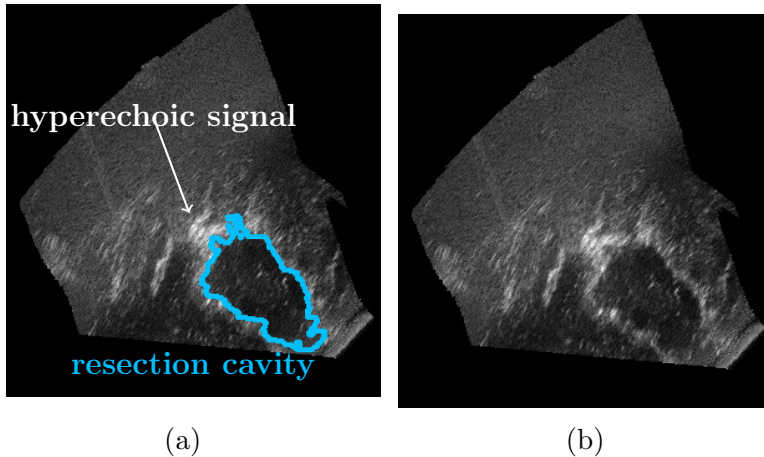


Figure 1: Ultrasound image of a resection cavity (a) with and (b) without segmentation.

157 without complete removal. Hyperechoic signals surrounding cavities in iUS images result  
 158 from sound attenuation differences between brain tissue and saline water, as well as the  
 159 presence of blood (see Fig. 1)<sup>30</sup>. To prevent false positives, only homogeneous, dark signals  
 160 were considered as cavities, potentially leading to slight underestimation in cases involving  
 161 blood-filled cavities. In challenging cases with small, entirely blood-filled cavities, segmen-  
 162 tation was not possible due to indistinguishable borders. For example, in three exceptional  
 163 instances (Case 11 during and after resection, and Case 15 during resection), the cavities  
 164 appeared notably small and completely inundated with blood, without any noticeable dark  
 165 signals.

166 It is worth noting that, due to the inherent variability in surgical procedures, determin-  
 167 ing the precise timing of image capture was challenging since it could occur at different stages  
 168 of the resection process. The crucial factor was ensuring that US images were taken before  
 169 the surgeon completed the resection entirely, even if residual tumors remained. The segmen-  
 170 tation of resection cavities was conducted using ITK-SNAP<sup>28</sup>. Initially, regularly spaced  
 171 slices, approximately one in every five slices, were manually delineated. Subsequently, ITK's  
 172 morphological interpolation, facilitated by ITK-SNAP's Convert3D command-line tool, was  
 173 utilized to fill in the remaining slices. Convert3D is one of the companion tools of ITK-SNAP  
 174 that provides additional features. It is a command-line tool that enables the combination  
 175 of multiple image processing tasks into efficient mini-programs, making it an integral tool  
 176 in studies involving hundreds of 3D images. In cases where necessary, additional slices were  
 177 manually segmented to optimize the interpolation outcome. The segmentation process for  
 178 most RESECT cases was originally carried out by two raters as part of a previous study<sup>14</sup>.  
 179 Following an assessment of intra- and inter-rater variability, these segmentations were re-  
 180 viewed by a neurosurgeon and were then modified accordingly. Subsequently, for this study,  
 181 the remaining RESECT cases were segmented, and all cases underwent refinement during  
 182 the validation protocol detailed in section II.G..

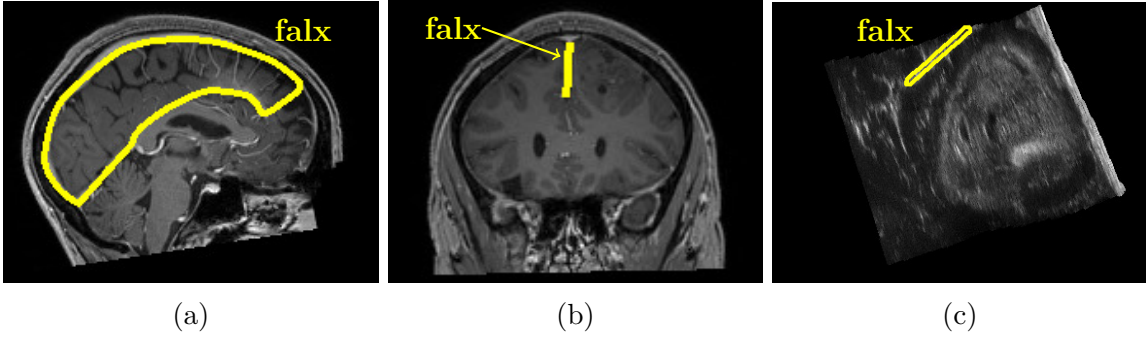


Figure 2: T1 MR (a), (b), and US (c) images of the falx cerebri.

## 183 II.D. iUS *Falx Cerebri* Segmentation Protocol

184 The *falx cerebri* is the membrane that separates the left and right hemispheres of the brain.  
 185 This cerebral falx has a hyperechoic signal in iUS images. It presents a characteristic quasi-  
 186 planar shape that appears as a straight line in coronal and axial slices. The falx is also visible  
 187 in the MR images, especially T1-weighted (Fig. 2). This structure is thus a convenient  
 188 landmark that can be particularly useful to anchor registration. The falx is not always  
 189 within the iUS volume due to the limited field of view but can be visible depending on the  
 190 tumor location. The falx segmentation is, therefore, present for some volumes only. Since  
 191 the falx' bright signal is similar to *sulci* it is difficult to localize the inferior border of the  
 192 membrane. We, therefore, used the registered T1-weighted MR images to adjust the falx  
 193 segmentation in height. Regularly spaced slices were manually delineated using ITK-SNAP  
 194 and then interpolated with Convert3D.

## 195 II.E. iUS *Sulci* Segmentation Protocol

196 For segmentation purposes, *sulci* were defined as folds filled with cerebrospinal fluid (CSF)  
 197 between brain tissue sections. CSF surrounding the brain, such as between the tissue and the  
 198 *dura mater* or *tentorium*, was not labeled, although it had a similar iUS signal. *Sulci* were  
 199 initially segmented with manual delineation every five slices and morphological interpolation  
 200 using Convert3D when moving through the volume in a single direction (e.g., axial slices).  
 201 Unlike volumetric structures, *sulci* are thin, complex, folded surfaces. To capture their  
 202 irregular shapes, each volume was annotated in three viewing directions (axial, sagittal, and  
 203 coronal), and these segmentations were first interpolated separately and later combined into  
 204 a union. While this process resulted in slight over-segmentation, it significantly improved  
 205 *sulci* delineation, according to annotators and neurosurgeons. In each case, the volume  
 206 preceding resection underwent segmentation aided by registered MR images to accurately  
 207 delineate *sulci* structures. This initial segmentation served as a reference for segmenting  
 208 the volume during and after resection. The manual segmentation process was facilitated by  
 209 ITK-SNAP, employing a Wacom One pen tablet, which demonstrated superior speed and  
 210 precision compared to a conventional computer mouse.

## 211 II.F. Pre-operative MR Tumor Segmentation

212 For completeness, we provide segmentations of the tumors in the pre-operative T2 FLAIR  
213 images. As the cases in the database are lower-grade gliomas, there is no contrast uptake in  
214 the T1 weighted images and the T2 FLAIR images are used to define the tumor boundaries.  
215 The tumors were semi-automatically segmented in 3DSlicer using the *GrowCut* algorithm<sup>31</sup>.  
216 The resulting segmentations were manually corrected when needed and smoothed with a  
217  $2 \times 2$  mm median filter.

## 218 II.G. Data Validation

219 All segmentations presented in this work were validated by two experienced neurosurgeons  
220 (S.D.R., O.S.). The segmentations were presented to the specialists through a case-by-  
221 case 3D Slicer scene, including the original iUS image, segmentation masks, and MR images.  
222 Figure 3 represents an example of such a scene. We asked specialists to grade all segmentation  
223 masks based on five criteria for three types of structures:

- 224 • Quality of tumor: smoothness of the boundaries (SMT), identification of tumoral tis-  
225 sues (IdT), exclusion of non-cancerous tissues (ExT)
- 226 • Quality of resection cavity: identification of resection cavity (IdR)
- 227 • Quality of *sulci* and falx: identification of sulci and falx (IdS)

228 The grading scheme for each criterion was on a scale of 1 to 5 defined as major improvement  
229 needed, minor improvement needed, acceptable, good quality, and excellent, respectively.  
230 For each criterion, a score of 3 from both surgeons was needed to pass the quality control  
231 of segmentation masks. Otherwise, the masks were revised according to the surgeons' com-  
232 ments. In determining the choice of a passing score of 3, it is important to clarify that this  
233 decision was rooted in the specific criteria established for surgeons evaluating the dataset.  
234 The selection of 3 as the pass score was deliberate, as it represented the midpoint on the  
235 validation scale of 1 to 5. This choice was informed by the summary of evaluation forms,  
236 aiming to identify a common rating among inter-rater assessments. Given the intricate and  
237 complex nature of brain structures, achieving consensus on a moderate score like 3 ensured  
238 a balanced assessment that accounted for the variability inherent in such evaluations. The  
239 final grades for each patient are presented in Table 1.

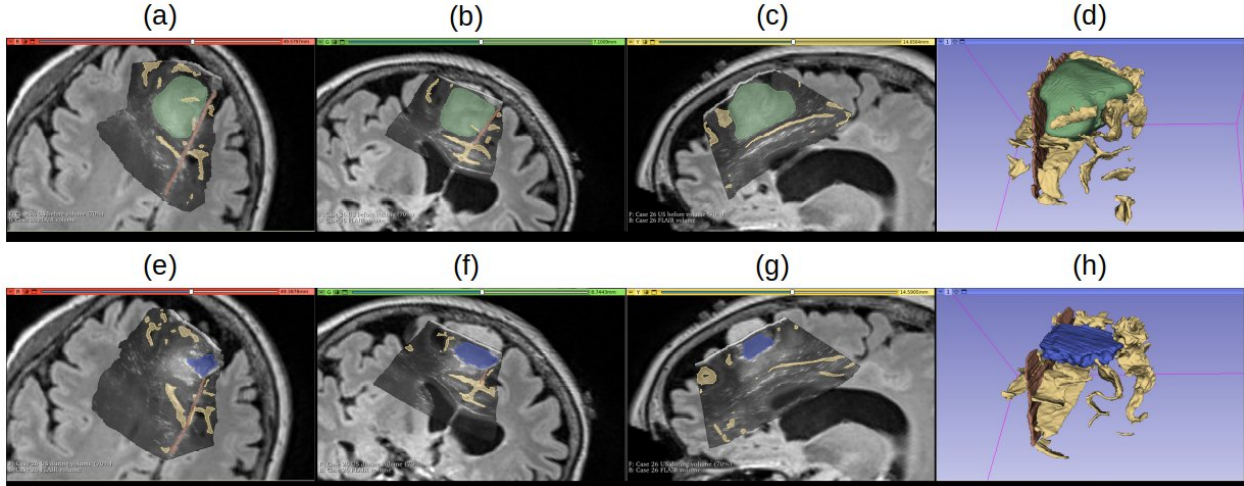


Figure 3: An example of segmentations overlaid with intra-operative ultrasound (iUS) and MR images (green: tumor; yellow: sulci; red: cerebral falx; blue: resection cavity). iUS volume before resection: (a)-(d); iUS volume during resection: (e)-(h).

### 240 III. Data Format and Usage Notes

241 The proposed RESECT-SEG segmentations are distributed in the NIFTI format. Upon the  
 242 acceptance of this paper, they will be available via the OSF open-science [https://osf.io/  
 243 jv8bk](https://osf.io/jv8bk) for public viewing and downloading and can be freely used by research laboratories  
 244 as well as clinical institutes. However, gaining any financial benefits from the distribution of  
 245 the proposed segmentation dataset is prohibited. The database is under the CC BY-NC-SA  
 246 4.0 License.

### 247 IV. Discussion

248 The border and shape of brain tumors have long been established as important diagnostic  
 249 markers in resection surgeries. Several image processing techniques have been adopted to  
 250 segment tumors which rely on the creation of mathematical descriptions of the tumor border.  
 251 Similarly, identifying resection cavity contours has been used to evaluate the completeness  
 252 of tumor resection. Finally, segmenting surrounding cerebral structures can greatly bene-  
 253 fit image analysis during the surgeries. However, validation of image processing techniques  
 254 needs to be investigated in the case of new data. It is important to highlight that there are  
 255 few brain datasets accessible to the public, and even those available, such as the BITE<sup>24</sup>,  
 256 RESECT<sup>25</sup>, and ReMIND<sup>26</sup> datasets, do not include iUS segmentation of brain anatomies.  
 257 The absence of US segmentation datasets for the brain is largely attributed to the complexity  
 258 of the task. To this end, we have provided the manual segmentations of cerebral structures  
 259 in iUS images of the 23-patient RESECT dataset, verified by two expert surgeons through  
 260 detailed evaluation criteria per brain anatomy. Our proposed expert-annotated RESECT-

261 SEG dataset comprises the segmentation masks of brain tumors, resection cavities, the *falx*  
 262 *cerebri*, and *sulci*. Tumor segmentations of the pre-operative MR images are also provided  
 263 as a reference. To the best of our knowledge, this is the first study that publicly provides a  
 264 comprehensive expert-annotation segmentation of iUS images. The challenging procedure of  
 265 delineating brain iUS images has impeded the publications of such segmentations. This vali-  
 266 dated dataset serves as a crucial asset for evaluating and benchmarking various segmentation  
 267 methods, thereby driving advancements in brain imaging research.

Table 1: Quality control grade chart for segmentation masks before, during, and after resection. Grades of the two neurosurgeons are given side-by-side in each cell. For Case 11 (during and after resection) and Case 15 (during resection), the resection cavity was not labeled (see section II.C).

Validation Scores								
Patient ID	Before Resection				During Resection		After Resection	
	SMT	IdT	ExT	IdS	IdR	IdS	IdR	IdS
1	4 4	4 5	4 3	3 4	3 3	4 4	3 4	4 4
2	4 4	4 3	3 5	4 4	3 4	4 4	3 5	4 5
3	4 4	3 3	4 3	3 3	3 4	3 3	4 4	4 3
4	3 4	3 5	4 5	3 4	3 4	4 4	4 5	3 4
5	3 4	4 4	4 4	3 4	3 5	3 4	4 5	4 3
6	3 4	4 5	3 5	3 4	4 5	4 4	4 5	4 4
7	3 4	3 5	4 4	3 4	3 3	4 4	4 5	4 4
8	4 3	4 4	4 5	3 4	3 5	3 4	3 5	4 4
11	4 4	4 4	3 5	4 4	- -	4 3	- -	4 3
12	3 4	4 3	4 3	4 4	3 4	3 4	4 5	4 5
13	4 4	4 4	3 4	4 3	3 5	4 5	3 5	4 3
14	4 4	3 4	4 4	4 4	4 3	4 4	4 4	3 4
15	3 4	3 3	4 3	4 4	- -	4 4	4 4	4 4
16	4 4	4 4	4 4	4 4	3 4	4 4	3 4	3 4
17	3 4	4 5	4 5	4 4	4 5	4 4	3 4	4 4
18	4 4	3 4	3 4	4 4	3 4	3 4	3 5	3 5
19	3 4	3 5	3 5	4 3	3 5	3 5	3 5	4 4
21	3 4	3 4	4 4	3 4	4 5	4 4	4 5	4 4
23	3 4	3 5	3 5	3 4	3 3	4 4	3 5	4 4
24	4 4	4 4	3 5	3 5	3 4	4 4	3 4	4 4
25	4 4	3 4	3 4	3 4	4 3	3 4	3 4	3 3
26	4 5	4 5	3 5	3 5	3 5	3 5	3 5	3 3
27	4 5	3 3	3 5	4 4	3 3	3 4	3 5	3 4

SMT: smoothness of the boundaries, IdT: identification of tumoral tissues, ExT: exclusion of non-cancerous tissues, IdS: identification of sulci and falx. IdR: identification of resection cavity

268 The proposed RESECT-SEG dataset offers substantial utility, focusing primarily on  
 269 two pivotal applications that have the potential to revolutionize brain tumor diagnosis and

270 treatment. As the first application, it accelerates the development of advanced image analy-  
271 sis algorithms for brain tumor detection and segmentation, whether based on deep learning  
272 or energy minimization. With the growing number of segmentation algorithms, there is  
273 a need for comprehensive evaluation, and this dataset provides a standardized metric for  
274 rigorous testing, propelling advancements in brain cancer treatment. Therefore, the pro-  
275 posed dataset offers an opportunity for both technical and clinical communities to rigor-  
276 ously test their algorithms. Additionally, it offers a unique opportunity for algorithms to  
277 excel in multi-instance detection and segmentation, enhancing performance beyond binary  
278 segmentation tasks. Multiple methodologies are available for binary segmentation problems;  
279 however, recent studies suggest that integrating instances into deep learning algorithms not  
280 only enhances performance through parallel multi-instance segmentation but also achieves  
281 a comprehensive improvement overall<sup>32</sup>. Consequently, this dataset acts as a catalyst in  
282 refining computer-aided diagnosis (CAD) systems, enabling multi-instance and multi-organ  
283 analyses, thereby revolutionizing brain tumor diagnosis and treatment.

284 The second application is transformative, focusing on developing and validating  
285 segmentation-based registration algorithms to address brain shift challenges during surgery.  
286 Brain shift, involving tissue deformation and displacement, poses precision hurdles in surgery.  
287 Integrating this dataset into registration algorithms provides them with expert-annotated  
288 tumor segmentations as a foundation. These resources empower algorithms to dynamically  
289 recalibrate pre-operative images in real-time, aligning them with evolving intraoperative con-  
290 ditions. The result is an advanced neuronavigation system, offering surgeons accurate, real-  
291 time patient anatomical visualization. This leads to enhanced resection control, minimizing  
292 structural damage risk and optimizing tumor removal. The synergy between segmentation  
293 and registration algorithms has the potential to redefine neurosurgery, equipping surgeons  
294 with a powerful tool to navigate brain shift complexities, ultimately ensuring safer surgeries,  
295 better patient outcomes, and improved resection control. This advancement holds promise  
296 for revolutionizing the field of neurosurgery.

297 The proposed RESECT-SEG dataset stands as a pivotal resource for advancing image  
298 processing techniques in neurosurgery. While it offers valuable segmentations of cerebral  
299 structures, it's essential to acknowledge its limitations. One such concern is the potential  
300 lack of representation of diverse clinical scenarios. Ensuring the dataset encapsulates a broad  
301 spectrum of anatomical variations, tumor types, and imaging modalities is crucial for its  
302 relevance and applicability in broader contexts. Evaluating the generalizability of proposed  
303 techniques beyond the confines of the RESECT-SEG dataset is imperative. Nevertheless,  
304 by adhering to rigorous evaluation protocols, conducting thorough validation processes, and  
305 maintaining transparent reporting standards, the RESECT-SEG dataset can significantly  
306 improve its credibility and impact in advancing neurosurgical image processing techniques.

## 307 V. Conclusion

308 In this study, the most comprehensive and validated expert delineations of cerebral structures  
309 within iUS images from the RESECT database were proposed. The primary focus lay in

310 outlining tumor boundaries within pre-resection iUS 3D volumes and tracking the resection  
311 cavity both during and post-surgery. Additionally, delineated *sulci* and the *falx cerebri* were  
312 further provided to enhance surgical precision. This dataset presents an invaluable resource  
313 for both the training and evaluation of DL-based segmentation algorithms and registration  
314 methodologies, thereby presenting a rigorous challenge to their capabilities. This collective  
315 effort is poised to catalyze advancements in brain tumor treatment and surgical interventions,  
316 ultimately benefiting patients and furthering the realm of medical science.

## 317 Acknowledgements

318 This work has been supported by the Natural Sciences and Engineering Research Council  
319 of Canada (NSERC), the French National Research Agency through the frameworks Com-  
320 puter Assisted Medical Interventions (ANR-11-LABX-0004 CAMI Labex) and the Multidis-  
321 ciplinary Institute in Artificial Intelligence (ANR-19-P3IA-0003 MIAI@Grenoble Alpes).

## 322 References

- 324 <sup>1</sup> D. N. Louis, A. Perry, P. Wesseling, D. J. Brat, I. A. Cree, D. Figarella-Branger,  
325 C. Hawkins, H. K. Ng, S. M. Pfister, G. Reifenberger, R. Soffietti, A. von Deimling,  
326 and D. W. Ellison, The 2021 WHO Classification of Tumors of the Central Nervous  
327 System: a summary, *Neuro-Oncology* **23**, 1231–1251 (2021).
- 328 <sup>2</sup> A. Omuro and L. M. DeAngelis, Glioblastoma and other malignant gliomas: a clinical  
329 review, *Jama* **310**, 1842–1850 (2013).
- 330 <sup>3</sup> T. Schneider, C. Mawrin, C. Scherlach, M. Skalej, and R. Firsching, Gliomas in adults,  
331 *Deutsches Ärzteblatt International* **107**, 799 (2010).
- 332 <sup>4</sup> I. J. Gerard, M. Kersten-Oertel, J. A. Hall, D. Sirhan, and D. L. Collins, Brain Shift in  
333 Neuronavigation of Brain Tumors: An Updated Review of Intra-Operative Ultrasound  
334 Applications, *Frontiers in Oncology* **10** (2021).
- 335 <sup>5</sup> A. Nabavi et al., Serial intraoperative magnetic resonance imaging of brain shift, *Neu-  
336 rosurgery* **48**, 787–798 (2001).
- 337 <sup>6</sup> I. Reinertsen, D. L. Collins, and S. Drouin, The essential role of open data and software  
338 for the future of ultrasound-based neuronavigation, *Frontiers in Oncology* **10**, 3219  
339 (2021).
- 340 <sup>7</sup> D. C. D. A. Bastos, P. Juvekar, Y. Tie, N. Jowkar, S. Pieper, W. M. Wells, W. L. Bi,  
341 A. Golby, S. Frisken, and T. Kapur, Challenges and Opportunities of Intraoperative  
342 3D Ultrasound With Neuronavigation in Relation to Intraoperative MRI, *Frontiers in  
343 Oncology* **11**, 1463 (2021).

- 344 <sup>8</sup> U. Yeole, V. Singh, A. Mishra, S. Shaikh, P. Shetty, and A. Moiyadi, Navigated intraop-  
345 erative ultrasonography for brain tumors: a pictorial essay on the technique, its utility,  
346 and its benefits in neuro-oncology, *Ultrasonography* **39**, 394 (2020).
- 347 <sup>9</sup> J. Zhang, X. Chen, Y. Zhao, F. Wang, F. Li, and B. Xu, Impact of intraoperative mag-  
348 netic resonance imaging and functional neuronavigation on surgical outcome in patients  
349 with gliomas involving language areas, *Neurosurgical review* **38**, 319–330 (2015).
- 350 <sup>10</sup> D. C. d. A. Bastos, P. Juvekar, Y. Tie, N. Jowkar, S. Pieper, W. M. Wells, W. L. Bi,  
351 A. Golby, S. Frisken, and T. Kapur, A Clinical Perspective on the Use of Intraoperative  
352 3D Ultrasound with Neuronavigation and Intraoperative MRI, *Frontiers in Oncology*  
353 **11**, 1463 (2021).
- 354 <sup>11</sup> A. Šteňo, J. Buvala, V. Babková, A. Kiss, D. Toma, and A. Lysak, Current Limitations  
355 of Intraoperative Ultrasound in Brain Tumor Surgery, *Frontiers in Oncology* **11**, 851  
356 (2021).
- 357 <sup>12</sup> J. Rubin, M. Mirfakhraee, E. Duda, G. Dohrmann, and F. Brown, Intraoperative ultra-  
358 sound examination of the brain., *Radiology* **137**, 831–832 (1980).
- 359 <sup>13</sup> R. Sastry, W. L. Bi, S. Pieper, S. Frisken, T. Kapur, W. Wells III, and A. J. Golby,  
360 Applications of ultrasound in the resection of brain tumors, *Journal of Neuroimaging*  
361 **27**, 5–15 (2017).
- 362 <sup>14</sup> F.-X. Carton, M. Chabanas, F. Le Lann, and J. H. Noble, Automatic segmentation  
363 of brain tumor resections in intraoperative ultrasound images using U-Net, *Journal of*  
364 *Medical Imaging* **7**, 1 – 15 (2020).
- 365 <sup>15</sup> A. I. Namburete, W. Xie, M. Yaqub, A. Zisserman, and J. A. Noble, Fully-automated  
366 alignment of 3D fetal brain ultrasound to a canonical reference space using multi-task  
367 learning, *Medical Image Analysis* **46**, 1–14 (2018).
- 368 <sup>16</sup> E. Ilunga-Mbuyamba, J. G. Avina-Cervantes, D. Lindner, F. Arlt, J. F. Ituna-Yudonago,  
369 and C. Chalopin, Patient-specific model-based segmentation of brain tumors in 3D  
370 intraoperative ultrasound images, *International journal of computer assisted radiology*  
371 *and surgery* **13**, 331–342 (2018).
- 372 <sup>17</sup> L. Canalini, J. Klein, D. Miller, and R. Kikinis, Segmentation-based registration of  
373 ultrasound volumes for glioma resection in image-guided neurosurgery, *International*  
374 *journal of computer assisted radiology and surgery* **14**, 1697–1713 (2019).
- 375 <sup>18</sup> L. Canalini, J. Klein, D. Miller, and R. Kikinis, Enhanced registration of ultrasound  
376 volumes by segmentation of resection cavity in neurosurgical procedures, *International*  
377 *Journal of Computer Assisted Radiology and Surgery* **15**, 1963–1974 (2020).
- 378 <sup>19</sup> F. Milletari, S. Ahmadi, C. Kroll, A. Plate, V. E. Rozanski, J. Maiostre, J. Levin,  
379 O. Dietrich, B. Ertl-Wagner, K. Bötzel, and N. Navab, Hough-CNN: Deep Learning for  
380 Segmentation of Deep Brain Regions in MRI and Ultrasound, *CoRR* **abs/1601.07014**  
381 (2016).

- 382 <sup>20</sup> Z. Li, K. Kamnitsas, and B. Glocker, Overfitting of neural nets under class imbalance:  
383 Analysis and improvements for segmentation, in *International Conference on Medical*  
384 *Image Computing and Computer-Assisted Intervention*, pages 402–410, Springer, 2019.
- 385 <sup>21</sup> H. Spitzer, K. Kiwitz, K. Amunts, S. Harmeling, and T. Dickscheid, Improving cytoar-  
386 chitectonic segmentation of human brain areas with self-supervised siamese networks,  
387 in *International Conference on Medical Image Computing and Computer-Assisted Inter-*  
388 *vention*, pages 663–671, Springer, 2018.
- 389 <sup>22</sup> N. Tajbakhsh, L. Jeyaseelan, Q. Li, J. N. Chiang, Z. Wu, and X. Ding, Embracing  
390 imperfect datasets: A review of deep learning solutions for medical image segmentation,  
391 *Medical Image Analysis* **63**, 101693 (2020).
- 392 <sup>23</sup> B. H. Menze et al., The multimodal brain tumor image segmentation benchmark  
393 (BRATS), *IEEE transactions on medical imaging* **34**, 1993–2024 (2014).
- 394 <sup>24</sup> L. Mercier, R. F. Del Maestro, K. Petrecca, D. Araujo, C. Haegelen, and D. L. Collins,  
395 Online database of clinical MR and ultrasound images of brain tumors, *Medical physics*  
396 **39**, 3253–3261 (2012).
- 397 <sup>25</sup> Y. Xiao, M. Fortin, G. Unsgård, H. Rivaz, and I. Reinertsen, RE troSpective Eval-  
398 uation of Cerebral Tumors (RESECT): A clinical database of pre-operative MRI and  
399 intra-operative ultrasound in low-grade glioma surgeries, *Medical physics* **44**, 3875–3882  
400 (2017).
- 401 <sup>26</sup> P. Juvekar et al., ReMIND: The Brain Resection Multimodal Imaging Database,  
402 medRxiv (2023).
- 403 <sup>27</sup> B. K. R. Munkvold, H. K. Bø, A. S. Jakola, I. Reinertsen, E. M. Berntsen, G. Unsgård,  
404 S. H. Torp, and O. Solheim, Tumor Volume Assessment in Low-Grade Gliomas: A  
405 Comparison of Preoperative Magnetic Resonance Imaging to C oregistered Intraopera-  
406 tive 3-Dimensional Ultrasound Recordings, *Neurosurgery* **83**, 288–296 (2018).
- 407 <sup>28</sup> P. A. Yushkevich, J. Piven, H. Cody Hazlett, R. Gimpel Smith, S. Ho, J. C. Gee, and  
408 G. Gerig, User-Guided 3D Active Contour Segmentation of Anatomical Structures:  
409 Significantly Improved Efficiency and Reliability, *Neuroimage* **31**, 1116–1128 (2006).
- 410 <sup>29</sup> A. Fedorov et al., 3D Slicer as an image computing platform for the Quantitative Imaging  
411 Network, *Magnetic resonance imaging* **30**, 1323–1341 (2012).
- 412 <sup>30</sup> T. Selbekk, A. Jakola, O. Solheim, T. F. Johansen, F. Lindseth, I. Reinertsen, and  
413 G. Unsgard, Ultrasound imaging in neurosurgery: approaches to minimize surgically  
414 induced image artefacts for improved resection control, *Acta Neurochir* **155** (2013).
- 415 <sup>31</sup> J. Egger, T. Kapur, A. Fedorov, S. Pieper, J. Miller, H. Veeraraghavan, B. Freisleben,  
416 A. Golby, C. Nimsky, and R. Kikinis, GBM volumetry using the 3D Slicer medical image  
417 computing platform. *Sci Rep* 3: 1364, 2013.

418 <sup>32</sup> C. Chen, B. Wang, C. X. Lu, N. Trigoni, and A. Markham, A survey on deep learning  
419 for localization and mapping: Towards the age of spatial machine intelligence, arXiv  
420 preprint arXiv:2006.12567 (2020).